

## Radiolysis of Quercetin in Methanol Solution: Observation of Depside Formation

ABDELGHAFOUR MARFAK,<sup>†</sup> PATRICK TROUILLAS,<sup>†</sup> DAOVY-PAULETTE ALLAIS,<sup>‡</sup>  
 YVES CHAMPAVIER,<sup>§</sup> CLAUDE-ALAIN CALLISTE,<sup>†</sup> AND JEAN-LUC DUROUX<sup>\*,†</sup>

UPRES EA 1085, Biomolécules et Cibles Cellulaires Tumorales, Faculté de Pharmacie,  
 University of Limoges, 2 rue du Dr. Marcland, 87025 Limoges Cedex, France

Radiolysis of the flavonol quercetin, a natural antioxidant, was performed in methanol. The degradation process was followed by HPLC analyses. The major product was identified as a depside (Q1) by NMR and LC–MS. The G(Q1) radiolytic factor was plotted versus the initial concentration of quercetin. This radiolytic process was attributed to the CH<sub>3</sub>O• radicals presented in the irradiated medium. The proposed mechanism invoked a stereospecific oxidation of the 3-hydroxyl group of quercetin which led to C-ring opening and to the formation of the depside Q1. In presence of water, Q1 was transformed into another depside, Q2, by an inverse esterification reaction. A chemical equilibrium was observed between Q1 and Q2. The comprehension of the radiolytic process of quercetin in methanol solution is of importance. Indeed, the same type of oxidative reactions could occur on flavonoids during preservation of food by ionizing radiation.

**KEYWORDS:** Quercetin; gamma irradiation; depsides; radiolytic mechanism

### INTRODUCTION

$\gamma$ -Irradiation process is used for food preservation. Recently this method has been investigated for fruits, but little is known about the modification of constitutive compounds. Because of the importance of flavonoids in human diet, it seems to be important to develop knowledge of  $\gamma$ -irradiation–flavonoid interaction.

The flavonoids are widely distributed in plants, especially in the skins and seeds of fruits and vegetables. Because of their presence in human food (1, 2), a large number of experimental studies on the potential health effect of diets rich in flavonoids has been carried out during the last 10 years (3). The flavonol quercetin has been the most studied flavonoid. One of its major interesting properties is antioxidant activity via free radical scavenging or iron chelation (4–7). It has also been shown that quercetin has multiple biological and pharmacological activities, including antiviral (8), antiinflammatory (9–11), anti-allergy, and anticancer properties (12–14).

None of the studies presented so far in the literature have discussed the effect of  $\gamma$ -irradiation on the flavonol quercetin. The degradation process of molecules in solution could be due to indirect oxidation–reduction reactions generated by the reactive species formed during the radiolysis of the solvent. In the present study, we investigated the effect of  $\gamma$ -irradiation on quercetin in methanol solutions. The degradation process of

quercetin was followed by HPLC analyses of the irradiated quercetin solutions.

### MATERIALS AND METHODS

**Chemicals and Reagents.** Methanol (HPLC grade, 99.8%) was purchased from SdS (Peypin, France), acetic acid was purchased from Merck (Darmstadt, Germany), and quercetin was from Sigma (St. Louis, MO).

**Irradiation Treatment.** Different solutions of quercetin dissolved in methanol were prepared, and were irradiated in aliquots of 1 mL with different doses (1–20 kGy) at a dose rate of 800 Gy/h in the <sup>60</sup>Co source carrier type Oris experimental irradiator.

**HPLC Analyses.** For each analysis of pure quercetin (5 × 10<sup>-5</sup> M, 10<sup>-4</sup> M, 5 × 10<sup>-4</sup> M, and 5 × 10<sup>-3</sup> M), as control, and irradiated quercetin, 20  $\mu$ L was injected into the analytical HPLC system, a Waters model equipped with a 600 model pump, a variable wavelength photodiode array detector (PDA 996), and a 600 model controller. The column used was a 250 × 4.6 mm i.d., 10  $\mu$ m,  $\mu$ Bondapak C18 cartridge (Waters). The mobile phase consisted of 100% methanol (A) and 1% aqueous acetic acid (B). Analyses were performed using a linear gradient from 20% A to 80% A during 40 min at 1 mL/min.

**Isolation Procedure of Products Q1 and Q2 Using Preparative HPLC.** A 5 × 10<sup>-3</sup> M solution of quercetin (48 mg) in methanol was irradiated at the dose of 14 kGy. The purification was performed by semipreparative HPLC using a 100 × 25 mm i.d., 10  $\mu$ m,  $\mu$ Bondapak C18 cartridge (Waters) and the same solvent system as above. The gradient was 20% A to 80% A at 5 mL/min during 60 min. The eluant containing Q1 was collected from 47 to 49 min and was evaporated at 45 °C under vacuum to give 9.4 mg. HPLC analysis was then carried out, indicating the presence of Q1 and a new compound named Q2. A second purification was done, giving 6.4 mg of product Q2.

**Identification of Products Q1 and Q2.** The identification was carried out by the NMR and LC–MS techniques. <sup>1</sup>H NMR and <sup>13</sup>C

\* To whom correspondence should be addressed. Phone: 33 5 55 43 58 45. Fax: 33 5 55 43 58 44. E-mail: duroux@pharma.unilim.fr.

<sup>†</sup> Laboratoire de Biophysique.

<sup>‡</sup> Laboratoire de Pharmacognosie.

<sup>§</sup> Service commun de RMN.

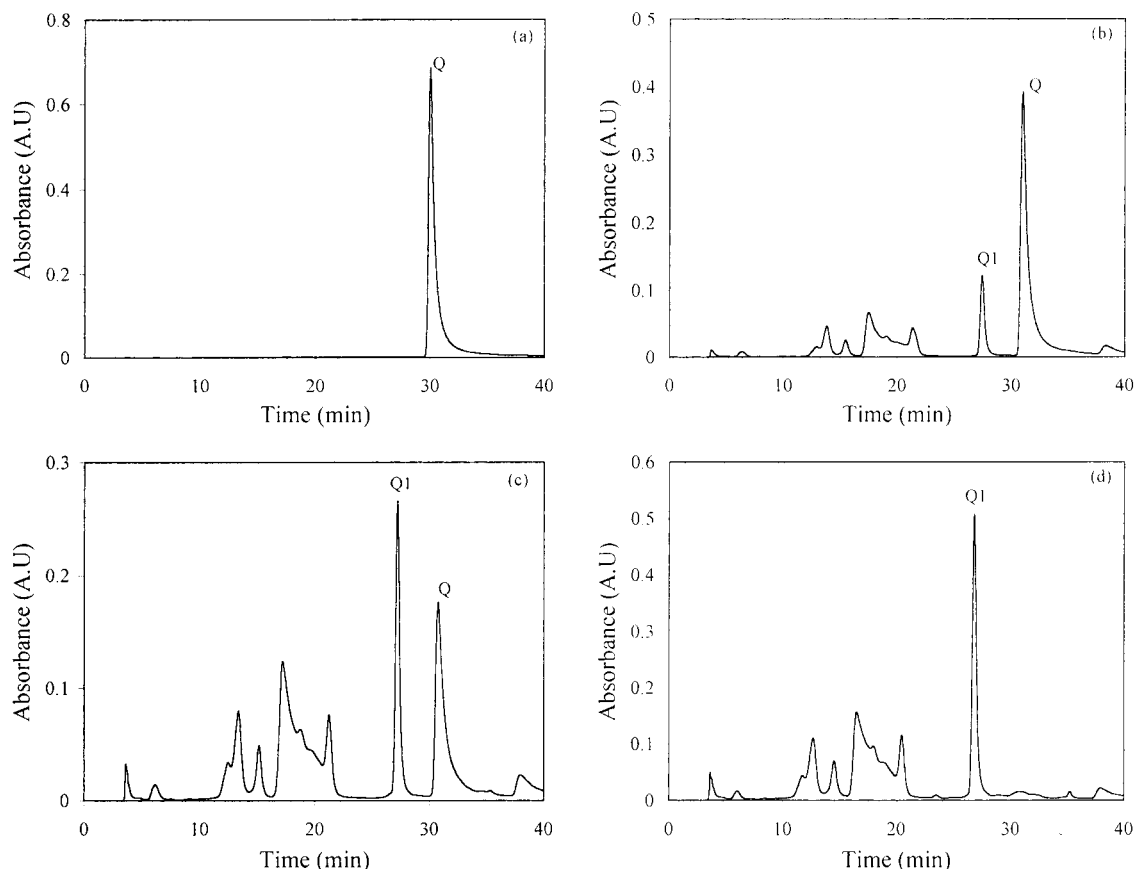


**Figure 1.** HPLC chromatograms, recorded at 280 nm, of quercetin (a) and irradiated quercetin ( $5 \times 10^{-3}$  M) at different doses: 4 kGy (b); 8 kGy (c); and 14 kGy (d).

NMR spectra were measured at 300 K in  $CD_3OD$  at 400 MHz for  $^1H$  NMR (dual probe) and 100 MHz for  $^{13}C$  NMR (dual probe) on a Bruker DPX Avance Spectrometer using tetramethylsilane as internal standard. The complete proton and carbon assignments were based on 1D ( $^1H$  standard,  $^{13}C$  Jmod) and 2D ( $^1H$ - $^1H$  correlation spectroscopy (COSY),  $^1H$ - $^{13}C$  heteronuclear multiple quantum coherence (HMQC), and  $^1H$ - $^{13}C$  heteronuclear multiple bond correlation (HMBC)) NMR experiments. Mass spectroscopy was performed on a Waters Alliance system equipped with a Waters electrospray interface. The source was operated in the negative and positive ions modes ( $ES^-$  and  $ES^+$ ) with a 40 V cone voltage.

## RESULTS AND DISCUSSION

**$\gamma$ -Irradiation of Quercetin.**  $\gamma$ -Irradiation of a methanol solution of quercetin was performed with different doses. The HPLC chromatograms of quercetin at a  $5 \times 10^{-3}$  M concentration, as control, and of irradiated quercetin at different radiation doses are shown in **Figure 1**. The quercetin peak ( $R_t = 30$  min) decreased when irradiation dose increased. For the high concentration ( $5 \times 10^{-3}$  M), the quercetin quantity decreased significantly between 2 kGy and 14 kGy, and beyond this irradiation dose, no significant differences were observed. We concluded that  $\gamma$  irradiation was able to degrade quercetin almost completely within 14 kGy at this concentration. In contrast, for low concentrations ( $<10^{-3}$  M), short times of irradiation treatment (dose  $<3$  kGy) were enough to degrade all molecules of the quercetin methanol solution.

**Figure 1b, c, and d** show the increase in new peaks, which indicate the formation of several compounds. The area of each peak increased while the quercetin one decreased. We determined the concentration of the major radiolytic compound eluted at  $R_t = 27$  min and which we called Q1. The concentrations

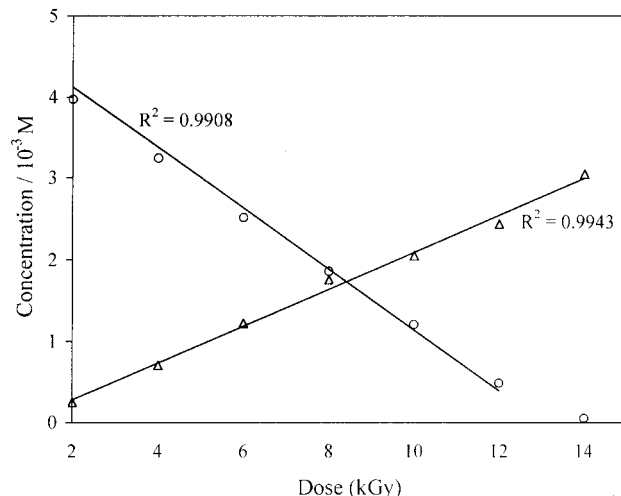


**Figure 2.** Change in concentration of Q (O) and Q1 ( $\Delta$ ) from a  $5 \times 10^{-3}$  M quercetin methanol solution irradiated at different doses of  $\gamma$ -ray at a dose rate of 800 Gy/h from  $^{60}Co$  source.

were calculated by the use of calibration curves made with purified materials.

**Figure 2** shows the change in the concentrations of Q1 and the consumption of quercetin versus the  $\gamma$ -irradiation doses, obtained from radiolysis of methanol quercetin solution ( $5 \times 10^{-3}$  M). A good linear relationship was observed ( $R^2 > 0.99$ ). The G-values of Q1 were determined from the slope of linear concentration-dose equations and with the formula (1) (15)

$$G = \frac{9.65 \times 10^6 \Delta M}{0.79 D} \quad (1)$$

where  $D$  is the dose (Gy),  $\Delta M$  is the concentration (mol/L) of the molecules formed, and  $G$  is the radiation chemical yield, which corresponds to the number of molecules liberated per 100 eV of absorbed energy.  $G$  is the parameter which characterizes the radiolysis efficiency of a product (15). The linear relationship, observed in **Figure 2**, indicated that  $G(Q1)$  was independent of the irradiation dose. This point confirmed that the experimental conditions chosen conformed with a "simple" model of radiolysis. All theoretical studies of solution radiolysis indicate that  $\gamma$ -rays interact with the molecules of the medium and form excited species and secondary electrons which are confined into small zones around the primary interaction, called "spurs" because of their 3D-geometrical configuration (15). Hence, heterogeneous zones appear along the track of the particles.  $G$  is constant when no overlapping of heterogeneous zones occurs, which is the case for low linear energy transfer (LET) radiation such as  $^{60}\text{Co}$   $\gamma$  rays, used at low doses and low solute concentrations. These conditions are required in order to not complicate the radiolysis process and its interpretation. Nevertheless, we observed, for high doses, saturation effects of  $G$  (data not shown) which could be attributed to saturation of the radical species formed in solvent or to overlapping phenomena along the track.

When we determined the  $G$  values versus the concentrations, we observed an increase of  $G$  when concentration increased.  $G$  seemed to saturate for concentrations higher than  $10^{-3}$  M. This evolution conformed with a "classic" radiolytic process (16), where the solute reacts with the radiolytic species from the solvent, until all substrate was consumed.

To understand the problem of the radiolysis of quercetin in solution, we had to consider different types of effects. First, direct effects could occur on solute molecules, leading to excitation and ionization of the molecules. Direct effects could occur with solutions at high concentration or with large molecules (polymers or DNA). In our case ( $\sim 10^{-3}$  M concentration of quercetin), direct effects could be considered only as a minor contribution. Second, indirect effects can be responsible for chemical degradation of the molecules. In this scheme, the solvent radiolysis products lead to chemical cascade events which yield some very reactive species. The radiolysis of methanol and some other alcohols has been established for many years (17). It was shown that 50 ns after the beginning irradiation, the irradiated solution becomes a homogeneous solution of reactive species, and if the concentration of the solute is small enough ( $< 5 \times 10^{-3}$  M), its degradation is activated only by these radical species. In the case of methanol radiolysis, the reactive homogeneous solution is composed by solvated electron ( $e_s^-$ ),  $\text{H}_2$ ,  $\text{H}^\bullet$ ,  $\text{CH}_3\text{O}^\bullet$ ,  $\bullet\text{CH}_2\text{OH}$ ,  $(\text{CH}_2\text{OH})_2$ ,  $\text{H}_2\text{CO}$ , and  $\text{H}^+$  such as  $\text{CH}_3\text{OH}_2^+$ . The strong potential for electron transfer by the cited species indicates that the degradation of the solute is a consequence of oxidation–reduction reactions, such as stereospecific oxidation, hydroxylation, and scission of molecules.

All of the reactions in solute are generally very fast and occur during the first second of the process. In the present study, it was interesting to notice that the chromatogram reached a definitive pattern for high doses, which indicated that the radiolysis products were stable against irradiation. However, after irradiation, we observed during the isolation of Q1, the formation of a second compound Q2 eluting at  $R_t = 12$  min (**Figure 3a**). It was clear that this chemical transformation occurred out of the irradiated medium and was not due to the irradiation process.

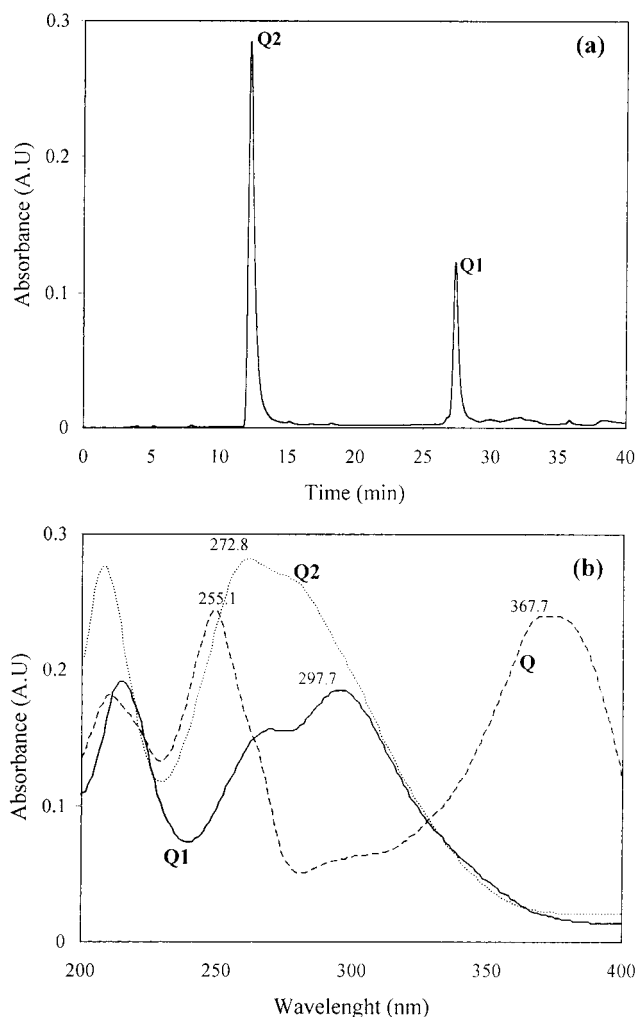


**Figure 3.** HPLC chromatogram obtained after evaporation of isolated product Q1 from  $5 \times 10^{-3}$  M quercetin methanol solution irradiated at 14 kGy (a), and the UV spectra of products Q1, Q2, and quercetin (Q) (b).

**UV/Vis Spectra of Q1 and Q2.** The UV spectra of the products (**Figure 3b**) exhibited two major absorption bands in the 222–227 nm range and in the 270–298 nm range. Compared to the UV spectrum of quercetin, we concluded that both the characteristic absorption bands at 255 nm and at 369 nm (attributed to the A–C ring conjugation and to the B–C ring conjugation, respectively) had disappeared. This indicated that in the Q1 and the Q2 structures, the C ring was destroyed.

**NMR and Mass Spectroscopic Identification of Q2 and Q1.** These two products were identified by  $^1\text{H}$ ,  $^{13}\text{C}$ , COSY, ROESY, NOESY, HMQC, and HMBC NMR experiments and by the negative and positive ES mass data.

The  $^1\text{H}$  NMR spectrum of product Q2 showed signals corresponding to five aromatic protons (**Table 1**). Two proton signals at 6.24 and 6.17 ppm possessed the same coupling constant ( $J = 2.2$  Hz) ascribable to the A-ring of quercetin, and a series of three proton signals at 7.58 ppm ( $d$ ,  $J = 2.1$  Hz), 7.56 ppm ( $dd$ ,  $J = 2.1, 8.2$  Hz), and 6.86 ppm ( $d$ ,  $J = 8.2$  Hz) were assigned to the B-ring of quercetin. The positions of all protons were confirmed by  $^1\text{H}$ – $^1\text{H}$  COSY spectra.

The  $^{13}\text{C}$  Jmod spectrum of Q2 showed three quaternary carbonyl groups, the first ascribable to a ketone function (188.6 ppm, C-7), the second ascribable to an acid group (165.8 ppm, C-8), and the third ascribable to an ester group (165.9 ppm, C-7'). The identification of these carbonyl groups was demonstrated by HMBC experiments (**Table 1**). Signals corresponding

**Table 1.**  $^1\text{H}$  (400 MHz) and  $^{13}\text{C}$  (100 MHz) NMR Data and Correlations Observed in COSY, HMQC, and HMBC Spectra of Products Q1 and Q2 in  $\text{CD}_3\text{OD}/\text{TMS}$  ( $\delta$  ppm;  $J$  Hz)

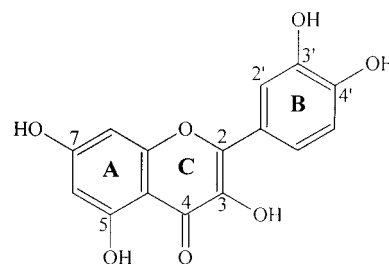
position	$^1\text{H}$	COSY	$^{13}\text{C}$ $J$ mod/ HMQC	HMBC
product Q1				
1			105.6	
2			168.2	
3	6.27 <i>d</i> (2.2)	H-5	101.7	C-1; C-2; C-4; C-5
4			167.7	
5	6.19 <i>d</i> (2.2)	H-5	105.0	C-1; C-3; C-4; C-6
6			155.4	
7			188.6	
8			165.5 <sup>a</sup>	
8-OCH <sub>3</sub>	3.44 s		53.2	C-8
1'			120.7	
2'	7.48 <i>d</i> (2.1)	H-6'	118.0	C-1'; C-3'; C-4'; C-6'; C-7'
3'			146.6	
4'			153.1	
5'	6.89 <i>d</i> (8.2)	H-6'	116.2	C-1'; C-3'; C-4'; C-6'
6'	7.50 <i>dd</i> (8.2; 2.1)	H-2'; H-5'	124.9	C-1'; C-2'; C-4'; C-5'; C-7'
7'			165.9 <sup>a</sup>	
product Q2				
1			105.5	
2			168.1	
3	6.24 <i>d</i> (2.2)	H-5	101.5	C-1; C-2; C-4; C-5
4			167.2	
5	6.17 <i>d</i> (2.2)	H-3	104.7	C-1; C-3; C-4; C-6
6			155.5	
7			188.6	
8			165.8 <sup>b</sup>	
1'			121.3	
2'	7.58 <i>d</i> (2.1)	H-6'	118.4	C-1'; C-3'; C-4'; C-6'; C-7'
3'			146.3	
4'			152.7	
5'	6.86 <i>d</i> (8.2)	H-6'	116.1	C-1'; C-3'; C-4'; C-6'
6'	7.56 <i>dd</i> (8.2; 2.1)	H-2'; H-5'	125.0	C-1'; C-2'; C-4'; C-5'; C-7'
7'			165.9 <sup>b</sup>	

<sup>a,b</sup> Assignments may be interchangeable.

to twelve aromatic carbons were also detected, five of which were tertiary (101.5 ppm, C-3; 104.7 ppm, C-5; 118.4 ppm, C-2'; 116.1 ppm, C-5'; 125.0 ppm, C-6') and seven of which were quaternary. Five of these latter were O-linked (168.1 ppm, C-2; 167.2 ppm, C-4; 155.5 ppm, C-6; 146.3 ppm, C-3'; 152.7 ppm, C-4'), and two were C-linked (105.5 ppm, C-1; 121.3 ppm, C-1'). The positions of the five tertiary carbons were assigned from the  $^1\text{H}$ – $^{13}\text{C}$  HMQC experiments (Table 1). These data confirmed the structure of the A-ring. In addition, the positions of all O-linked and C-linked aromatic carbons were deduced with the carbon–proton long-range couplings obtained from the HMBC spectrum (Table 1).

The ROESY and the NOESY experiments of Q2 were performed. No NOE correlations were observed between H3 and H6' or H2'. This result is not an indication of no connection between the two rings, but indicating that the stable conformation is obtained for torsion angles between the two rings which implicate a "high" distance ( $\geq 4$ – $5$  Å) between the cited protons. However, the connection is elucidated as the following. First, the chemical shift of C1' (121.3 ppm), which corresponds to a C-linked carbon, and the  $^3J$  correlation between C7' (165.9 ppm) and the protons H2' (7.58 ppm), H6' (7.56 ppm), led us to establish the C1'–C7' linkage. Second, C7' and C2 (168.1 ppm) were identified as an ester group and an O-linked carbon respectively, which allowed the C7'–O–C2 linkage.

The absence of long-range couplings in the HMBC spectrum between any protons and the C-7 (188.6 ppm) and C-8 (165.8 ppm) carbons, together with the presence of the quaternary C-linked carbon (105.5 ppm, C-1), led us to establish the C1–



Quercetin

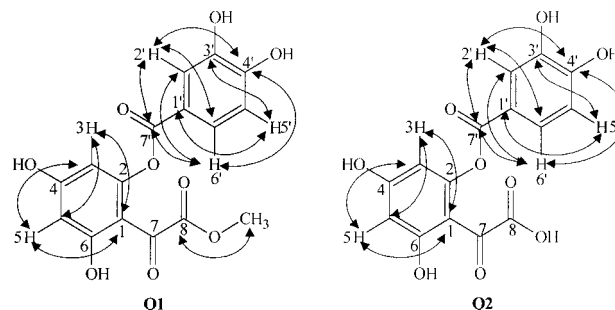


**Figure 4.** Selected  $^1\text{H}$ – $^{13}\text{C}$  long-range correlations ( $^3J$ ) ( $\leftrightarrow$ ) observed in HMBC spectra of products Q1 and Q2.

C7–C8 linkage. Finally, the product Q2 was identified as {2-[(3',4'-dihydroxybenzoyl)oxy]-4,6-dihydroxyphenyl}(oxo) acetic acid (Figure 4).

The negative and positive ES–MS spectra of product Q2 showed molecular ion peaks at  $m/z$  333  $[\text{M} - \text{H}]^-$  and at  $m/z$  357  $[\text{M} + \text{Na}]^+$ , respectively. The molecular weight of Q2 was determined to be 334, suggesting the formula  $\text{C}_{15}\text{H}_{10}\text{O}_9$ . The positive FAB–LSIMS mass spectroscopy, performed at Centre Régional de Mesures Physiques de l'Ouest (Rennes, France), using metanitrobenzyl alcohol (mNBA) matrix afforded pseudo molecular ion peak at  $m/z$  357  $[\text{M} + \text{Na}]^+$ . The high-resolution mode of the FABMS revealed that the molecular formula of Q2 was  $\text{C}_{15}\text{H}_{10}\text{O}_9$  (calculated for  $\text{C}_{15}\text{H}_{10}\text{O}_9\text{Na}$ , 357.0223; found, 357.0234) corresponding to the structure obtained from the NMR analysis. In addition, the positive ES–MS spectrum displayed other ion peaks at  $m/z$  137 and at  $m/z$  199 (Figure 5a). The presence of the  $m/z$  199 fragment confirms the C7–C8 linkage. The proposed pathways for these fragmentations are illustrated in Figure 6.

The  $^1\text{H}$  NMR and  $^{13}\text{C}$  spectra (Table 1) of product Q1 were found to be very similar to those of product Q2, and it appeared that they were of the same analogous series differing only by the presence of a methoxyl group, represented by a carbon resonance at 53.2 ppm, and by three protons (3.44 ppm, s). The chemical structure of Q1 was determined by procedures similar to those used for Q2 identification. The position of the methoxyl was determined by the observation of  $^3J$  correlation between the methoxyl protons (3.44 ppm) and the C-8 carbon (165.5 ppm). Consequently, the product Q1 was identified as {2-[(3',4'-dihydroxybenzoyl)oxy]-4,6-dihydroxyphenyl}(oxo) methyl acetate (Figure 4).

The observation of the molecular ions at  $m/z$  347  $[\text{M} - \text{H}]^-$ , at  $m/z$  349  $[\text{M} + \text{H}]^+$ , and at  $m/z$  371  $[\text{M} + \text{Na}]^+$ , respectively in the negative and positive ES–MS spectra, suggested the molecular formula  $\text{C}_{16}\text{H}_{12}\text{O}_9$  for Q1. The positive FAB–LSIMS mass spectroscopy, using metanitrobenzyl alcohol (mNBA) matrix, afforded pseudo molecular ion peaks at  $m/z$  349  $[\text{M} + \text{H}]^+$  and at  $m/z$  371  $[\text{M} + \text{Na}]^+$ . The high-resolution mode of the FABMS revealed that the molecular formula of Q1 was

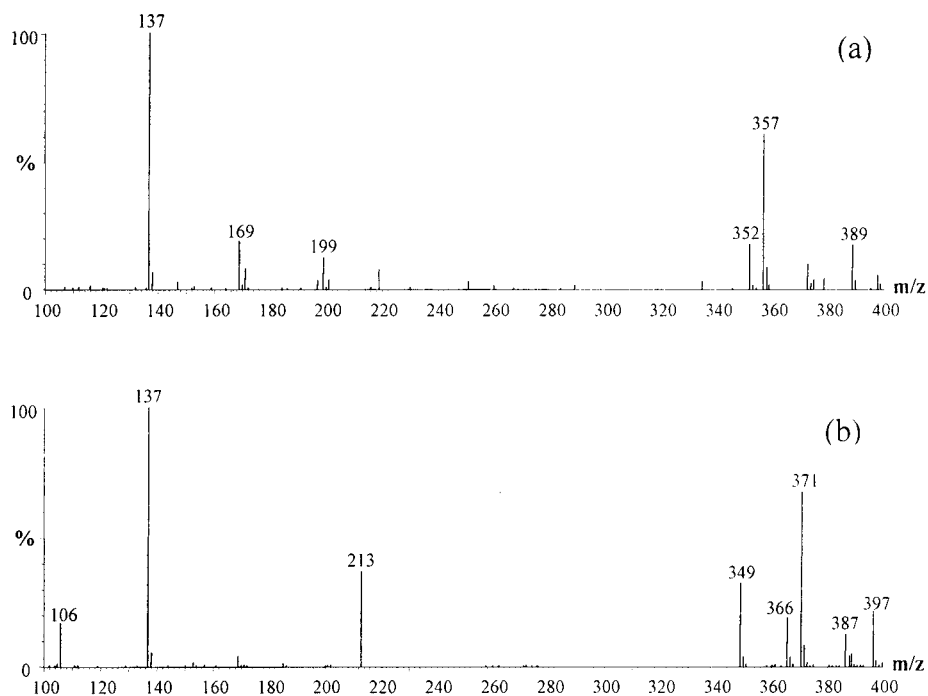


Figure 5. Positive ES-MS spectra of products Q2 (a) and Q1 (b).

$C_{16}H_{12}O_9$  (calculated for  $C_{16}H_{13}O_9$  and  $C_{16}H_{12}O_9Na$ , 349.0560 and 371.0379; found, 349.0560 and 371.0370, respectively) confirming the structure obtained from the NMR analysis.

Other fragment ions, in the positive spectrum, were detected at  $m/z$  137 and at  $m/z$  213 (Figure 5b). The proposed pathways of these fragments are illustrated in Figure 6. The fragment at  $m/z$  199 showed in the positive spectrum of the product Q2, was detected at  $m/z$  213 for the product Q1. This difference confirmed the  $-OCH_3$  group in Q1. In addition, the spectra of both Q1 and Q2 possessed the same fragment at  $m/z$  137, due to the same formation pathway of this fragment from Q1 and Q2.

**Equilibrium between Q1 and Q2.** In conclusion, the major radiolytic compound of Q is a depside. Formation of depsides during oxidation of flavonols has been proposed for many years (18) and was recently confirmed by oxidation catalyzed by flavonolato copper (II) phthalazine (19). However, Q1 seemed to be thermodynamically unstable under mild conditions, because it could be easily transformed in Q2 in the presence of water. Indeed, Q1 eluted in HPLC with approximately 70% MeOH/30% water. The water seemed to hydrolyze the methoxyl group and form Q2. When Q2 was dissolved in methanol, the esterification reaction was observed and the chemical equilibrium between Q1 and Q2 was established.

**Proposed Mechanism for Quercetin Radiolysis in Methanol Solution.** Quercetin is a flavonol and its antioxidant capacity is attributed to the presence of hydroxyl substituents in positions 3, 5, and 7 which permitted redox transfers, and to the  $\pi$  electron delocalization, between the B ring, the 2,3-double bond, and the keto group which was responsible for the stabilization of the radical produced during antioxidant reactions. Quercetin therefore exhibits a facility for oxidation-reduction reactions which occur during the radiolysis process. Aerial oxidation of flavonols has been established for many years. The primary process involved in quercetin oxidation is the opening of the 2,3-double bond with formation of the depside Q2 which is then hydrolyzed to the aromatic acids (18). In the case of quercetin radiolysis in methanol solution, we obtained the depside Q1 because, after opening the C ring, methoxylation was more easy

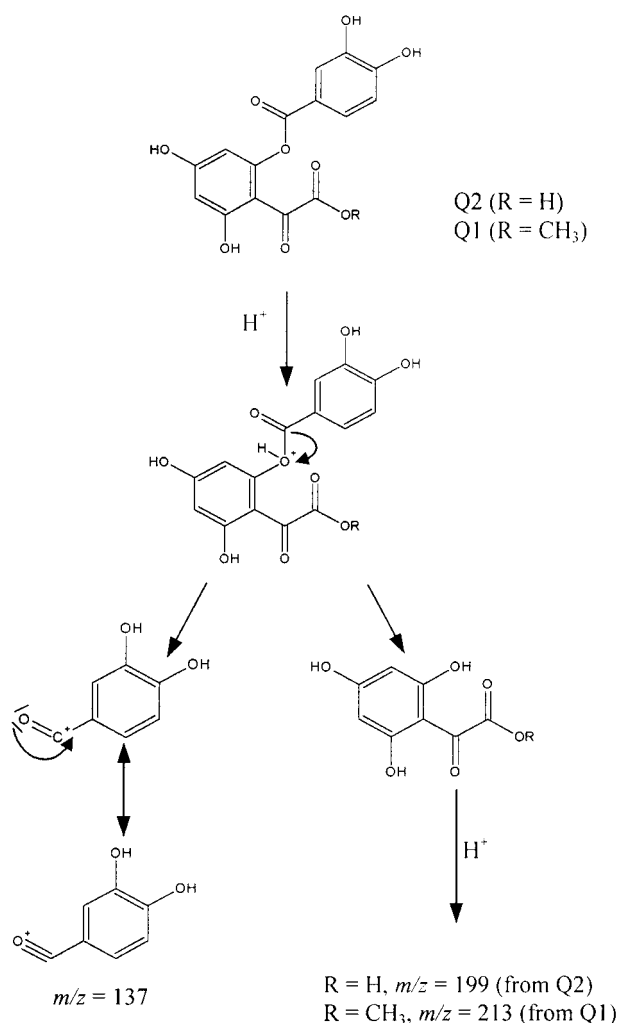


Figure 6. Proposed pathways for formation of the fragments at  $m/z$  213 and 137, detected in the positive ES-MS spectrum of the product Q1, and the fragments at  $m/z$  119 and 137, detected in that of compound Q2.

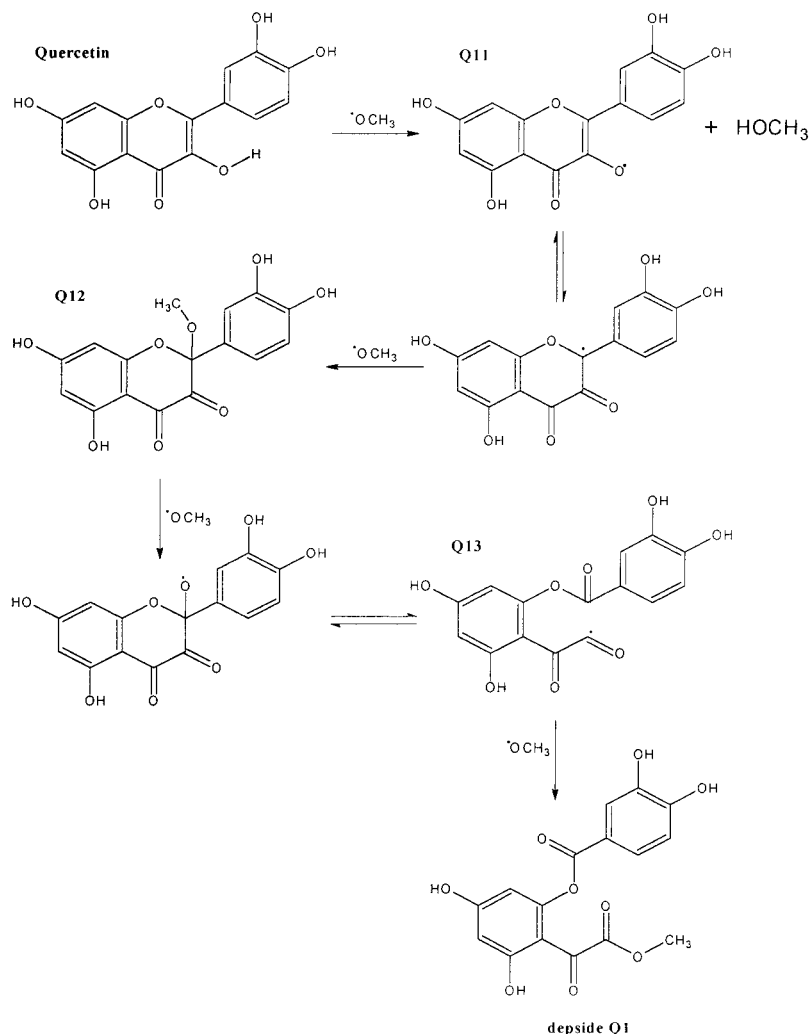


Figure 7. Proposed transformation mechanism for the formation of depside Q1 by  $\gamma$  radiolysis of quercetin.

than hydroxylation in radiolyzed methanol solution due to the presence of  $\cdot\text{OCH}_3$  radicals. We localized the primary reactive site of oxidation at position 3, because no irradiation product was formed after irradiation of rutin in the same experimental conditions used for quercetin. Rutin is quercetin glycosylated at position 3. We performed irradiation with doses up to 30 kGy and no effect was observed and concluded that sugar stabilized quercetin against oxidative reactions due to  $\gamma$  irradiation.

The transformation mechanism of quercetin to depside Q1 is shown in **Figure 7**. We propose that the  $\cdot\text{OCH}_3$  radicals, initiated by irradiation, react with the OH group in position 3 to form the flavonoxyl radical Q11. Then  $\cdot\text{OCH}_3$  radical could add to position 2 and form an intermediate product Q12. The  $\text{CH}_3$  of the methoxy group could then be eliminated from Q12 and the formation of a keto group in position 2 lead to scission of the molecule to compound Q13. Two mechanisms are proposed for  $\text{CH}_3$  elimination. First, a  $\text{H}\cdot$  radical could react with the  $\text{CH}_3$  group to form  $\text{CH}_4$ . The second mechanism implicates a  $\cdot\text{OCH}_3$  radical which yields the ether  $\text{CH}_3\text{OCH}_3$ . Such a mechanism seems to be more possible, because  $\cdot\text{OCH}_3$  was implicated in all the quercetin transformation steps we described in **Figure 7**. Probably because of their lifetime, the  $\cdot\text{OCH}_3$  radical must be the most likely candidate for these transformation reactions. Finally, a  $\cdot\text{OCH}_3$  radical reacts with the radical Q13 to form the depside Q1. The role of the OH groups in positions 3' and 4' seemed to be a minor factor in

formation of the major degradation product. However, it is possible that these groups reacted with the radicals of the irradiated medium to form some minor radiolytic compounds.

The irradiation process has been used to preserve the quality of food by killing bacteria, and so extend the shelf life (20, 21).  $\gamma$ -Irradiation has been reported as a potential treatment for extending the post-harvest life of fresh fruits and vegetables (22–24). It was also established that  $\gamma$ -irradiation of *Citrus clementina* Hort. ex. Tanaka increases the synthesis of total phenolic compounds including phenolic acids and flavonoids (25). However, little is known about the effect of  $\gamma$ -irradiation on the constitutive molecules of fruits and the vegetables, especially for flavonoids.  $\gamma$ -Irradiation of quercetin methanol solution does not constitute an exact model of flavonoid irradiation in fruits, however, it could contribute to the understanding of the reaction mechanism of quercetin with the free radicals produced in solution by irradiation. The free radicals produced in methanol and in acid water solution, which constitutes a better model of fruits, are not the same. Probably, the major oxidative species, during  $\gamma$ -irradiation of fruits, are produced from the water radiolysis. Pulsed radiolysis studies of flavonoids in water solution (26) reported stereospecific oxidation of the hydroxyl groups in B-ring. This process leads to the formation of the corresponding quinone. However, van Acker discussed the influence of pH on the oxidative sites in flavonoids (27). More generally, the structure–activity relationship studies showed that, according to the experimental condi-

tions, the oxidative site could be the 3-OH group, the 4-keto group, or the OH groups of B-ring (4, 5).

The chemical action of  $\cdot\text{OCH}_3$  observed probably does not mimic all the physical conditions which occur during fruit irradiation, but it constitutes the first step for investigating the radiolysis process, especially the C-ring opening. The flavonol scission was also obtained under favorable thermodynamic conditions such as in aerial oxidized solution (18) and catalytic reactions (28).

Because of the low water solubility of quercetin, and with the aim of reproducing the irradiation conditions of fruits, we actually try to irradiate quercetin methanol/water solutions.

#### ACKNOWLEDGMENT

We are grateful to H. Lotfi (Faculté de Pharmacie de Limoges, France) for his help in LC-MS measurements throughout this work.

#### LITERATURE CITED

- Herrmann, K. Flavonols and flavones in food plants: A review. *J. Food Technol.* **1976**, *11*, 433–448.
- Justesen, U.; Knuthsen, P.; Teth, T. Quantitative analysis of flavonols, flavones, and flavanones in fruits, vegetables and beverages by high-performance liquid chromatography with photodiode array and mass spectrometric detection. *J. Chromatogr. A* **1998**, *799*, 101–110.
- Hertog, M. G. L.; Feskens, E. J. M.; Hollman, P. C. H.; Katan, M. B.; Kromhout, D. Dietary antioxidant flavonoids and risk of coronary heart disease: The Zutphen elderly study. *Lancet* **1993**, *342*, 1007–1011.
- Pietta, P. G. Flavonoids as antioxidants. *J. Nat. Prod.* **2000**, *63*, 1035–1042.
- Rice-Evans, C. A.; Miller, N.; Paganga, G. Structure-antioxidant activity relationships of flavonoids and phenolic acids. *Free Radical Biol. Med.* **1996**, *20*, 933–956.
- Cotelle, N.; Bernier, J. L.; Catteau, J. P.; Pommery, J.; Wallet, J. C.; Gaydou, E. M. Antioxidant properties of hydroxy-flavones. *Free Radical Biol. Med.* **1996**, *20*, 35–43.
- Guohua, C.; Emin, S.; Ronald, L. Antioxidant and prooxidant behaviour of flavonoids: Structure-activity relationships. *Free Radical Biol. Med.* **1997**, *22*, 749–760.
- Van Hoof, L.; Van den Berghe, D. A.; Hatfield, G. M.; Vlietinck, A. J. Plant antiviral agents: V 3-Methoxyflavones as potent inhibitors of viral-induced block of cell synthesis. *Planta Med.* **1984**, *50*, 513–517.
- Brasseur, T. Anti-inflammatory properties in flavonoids. *J. Pharm. Belg.* **1989**, *44*, 235–241.
- Wei, B. L.; Lu, C. M.; Tsao, L. T.; Wang, J. P.; Lin, C. N. In vitro anti-inflammatory effects of quercetin 3-O-methyl ether and other constituents from *Rhamnus* species. *Planta Med.* **2001**, *67*, 745–747.
- Fischer, M.; Mills, G. D.; Slaga, T. J. Inhibition of mouse skin tumour promotion by several inhibitors of the arachidonic acid metabolism. *Carcinogenesis* **1982**, *3*, 1243–1245.
- Huang, M.; Ferraro, T. Phenolic compounds in foods and cancer prevention. In *Phenolic Compounds in Food and their Effect on Health II*, Huang, M. T., Ho, C. T., Lee, C. Y., Eds.; ACS Symposium Series; American Chemical Society: Washington, DC, 1992; Chapter 2, p 507.
- Huang, M. T.; Wood, A. W.; Newmark, H. L.; Sayer, J. M.; Yagi, H.; Jerina, D. M.; Conney, A. H. Inhibition of the mutagenicity bay-region diol-epoxides of polycyclic aromatic hydrocarbons by phenolic plant flavonoids. *Carcinogenesis* **1983**, *4*, 1631–1637.
- Sousa, R. L.; Marletta, M. A. Inhibition of cytochrom P-540 activity in rat liver microcosms by the naturally occurring flavonoid quercetin. *Arch. Biochem. Biophys.* **1985**, *240*, 345–357.
- Fricke, H.; Hart, E. J. Chemical dosimetry. In *Radiation Dosimetry*, Vol. II, Instrumentation; Attix, F. H., Roesch, W. C., Tochilin, E., Eds.; Academic Press: New York, 1966; pp 167–237.
- Ferrandini, C.; Pucheault, J. *Biologie de l'action des rayonnements*; Masson: Paris, 1983.
- Freeman, G. R., Ed. The radiolysis of alcohols. In *Kinetics of Nonhomogeneous Processes: A Practical Introduction for Chemists, Biologists, Physicists, and Materials Scientists*; Wiley-Interscience: New York, 1987; pp 73–101.
- Gottlieb, O. R. Flavonols. In *The Flavonoids*; Harborne, J. B., Mabry, T. J., Eds.; Chapman and Hall: London, 1975; pp 296–375.
- Balogh-Hergovich, E.; Kaiser, J.; Speier, G. Synthesis and characterization of copper (I) and copper (II) flavonolate complexes with phthalazine, and their oxygenation and relevance to quercetinase. *Inorg. Chim. Acta* **1997**, *256*, 9–14.
- Josephson, E. S.; Peterson, M. S. *Preservation of Food by Ionisation Radiation*. CRC Press: Boca Raton, FL, 1982; Vol. I–III.
- Zareena, A. V.; Variyar, P. S.; Gholap, A. S.; Bongirwar, D. R. Chemical investigation of gamma-irradiated saffron (*Crocus sativus* L.). *J. Agric. Food Chem.* **2001**, *49*, 687–691.
- Kader, A. A. Potential applications of ionizing radiation in postharvest handling of fresh fruits and vegetables. *Food Technol.* **1986**, *40*, 117–121.
- Urbain, W. M. Food irradiation. *Food Science Technology*; a series of monographs; Academic Press: Orlando, FL, 1986.
- Thomas, P. Radiation preservation of foods of plant origins Part VI. Mushrooms, tomatoes, minor fruits and vegetables, dried fruits and nuts. *CRC Crit. Rev. Food Sci. Nutr.* **1988**, *26*, 313–358.
- Oufedjikh, H.; Lacroix, M.; Mahrouz, M.; Amiot, M. J. Effect of  $\gamma$  irradiation on phenolic compounds and phenylalanine ammonia-lyase activity during storage in relation to peel injury from peel of *Citrus clementina* Hort. ex. Tanaka. *J. Agric. Food Chem.* **2000**, *48*, 559–565.
- Jovanovic, S. V.; Steenken, S.; Tosic, M.; Marjanovic, B.; Simic, M. G. Flavonoids as antioxidants. *J. Am. Chem. Soc.* **1994**, *116*, 4846–4851.
- Van Acker, S. A. B. E.; de Groot, M. J.; van den Berg, D. J.; Tromp, M. N. J. L.; den Kelder, G. D. O.; van der Vijgh, W. J. F.; Bast, A. A quantum chemical explanation of the antioxidant activity of flavonoids. *Chem. Res. Toxicol.* **1996**, *9*, 1305–1312.
- Kaiser, J.; Speier, G. Radical-initiated oxygenation of flavonols by dioxygen. *J. Mol. Catal. A* **2001**, *171*, 33–36.

---

Received for review February 7, 2002. Revised manuscript received May 28, 2002. Accepted May 30, 2002. This work was supported in part by the Ministère de l'Éducation Nationale, de la Recherche et de la Technologie and by the Conseil Régional du Limousin (France).